

---

# MoSE: Hierarchical Self-Distillation Enhances Early Layer Embeddings

---

Andrea Gurioli<sup>1</sup>, Federico Pennino<sup>1</sup>, Joao Monteiro<sup>2</sup>  
Maurizio Gabbrielli<sup>1</sup>

<sup>1</sup>University of Bologna, <sup>2</sup>Autodesk

Correspondence: andrea.gurioli5@unibo.it, joao.monteiro@autodesk.com

## Abstract

Deploying language models often requires navigating accuracy vs. performance trade-offs to meet latency constraints while preserving utility. Traditional model distillation reduces size but incurs substantial costs through training separate models. We introduce MODULARSTARENCODER (MOSE), a 1-billion-parameter multi-exit encoder for code retrieval and classification that employs a novel Self-Distillation mechanism. This approach significantly enhances lower-layer representations, enabling flexible deployment of different model portions with favorable performance trade-offs. Our architecture improves text-to-code and code-to-code search by targeting specific encoder layers as exit heads, where higher layers guide earlier ones during training—improving intermediate representations at minimal additional cost. We further enhance MOSE with a repository-level contextual loss that maximizes training context window utilization. Additionally, we release a new dataset created through code translation that extends text-to-code benchmarks with cross-language code-to-code pairs. Evaluations demonstrate the effectiveness of Self-Distillation as a principled approach to trading inference cost for accuracy across various code understanding tasks.

## 1 Introduction

Large language models (LLMs) have significantly impacted natural language processing (Niu et al., 2023), but their computational demands pose substantial deployment challenges. The field has responded with various efficiency strategies: quantization techniques reduce numerical precision (Jacob et al., 2017; Lin et al., 2023; Egiazarian et al., 2024); knowledge distillation trains smaller “student” models to emulate larger “teacher” models (Sanh et al., 2019; Jiao et al., 2019); and pruning methods eliminate less influential weights (Han et al., 2015). Concurrently, model families like LLAMA (Dubey et al., 2024), QWEN (Hui et al., 2024), MISTRAL (Jiang et al., 2023), and SMOLLM (Allal et al., 2025) exemplify a shift toward more efficient architectures at varying parameter scales.

Dynamic inference approaches further optimize efficiency through mechanisms like multi-exit networks. Early-exit architectures such as BRANCHYNET (Teerapittayanon et al., 2017) balance computation and accuracy by allowing predictions at intermediate layers, while Matryoshka representation learning (Kusupati et al., 2022) enables adjustment of computational complexity through embedding dimensionality pruning. These approaches maintain performance while reducing computational demands in resource-constrained environments. Furthermore, insights from the SimCLR framework (Chen et al., 2020) revealed that the final layer of a model does not necessarily produce the most semantically meaningful representations. Valeriani et al. (2023) analyzed the geometric evolution of hidden representations within large transformer models across layers, outlining that intermediate layers are identified as holding the most semantically rich representations for downstream tasks.

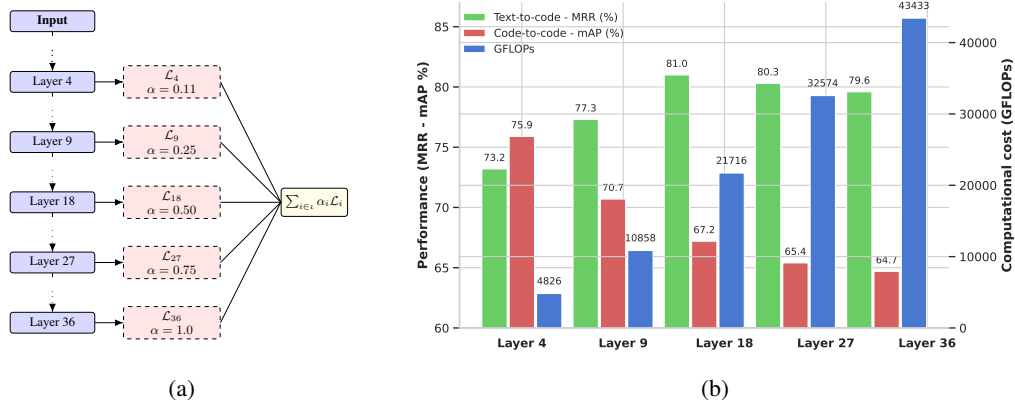


Figure 1: **(a)** Overview of our multi-exit self-distillation encoder, shown here with exit heads at selected layers (e.g., Layers 4, 9, 18, 27, and 36). Each exit head predicts an output embedding and adds a layer loss, contribution weighted by a coefficient  $\alpha_i$ , summed into the overall objective  $\mathcal{L}$ . **(b)** Computational cost (GFLOPs) vs. performances trade-off at different exit layers over CODESEARCHNET dataset (text-to-code in avg. MRR) and POJ104 (code-to-code in mAP). Despite a reduction of approximately 90% floating point operations from layer 36 to layer 4, MRR performance only drops by 6.4% in absolute terms. For POJ104, our best results are observed in the initial layers.

Building on these principles, we introduce MODULARSTARENCODER (MOSE), a modular multi-exit encoder built on top of the STARCODER-2 (Lozhkov et al., 2024) architecture, with 1 billion parameters that incorporate intra-model self-distillation. As illustrated in Figure 1a, our architecture applies training objectives at multiple exit points throughout the network (layers 4, 9, 18, 27, and 36), with each exit contributing a weighted loss component to the overall objective. This approach encourages lower layers to learn better representations by mimicking higher-layer outputs. Figure 1b demonstrates the resulting accuracy-computation trade-off of encoders trained under this framework: despite a 90% reduction in floating point operations from layer 36 to layer 4, performance over text-to-code retrieval drops by only 6.4% in absolute terms, while the model maintains the best performances for code-to-code retrieval in very early layers.

Notably, the exit point with the best performance isn’t necessarily the final layer, as noted in previous findings due to Chen et al. (2020); Valeriani et al. (2023). This offers both deployment flexibility and a natural model selection mechanism for specific tasks. Users can select which portion of the model to use during inference, starting from the first exit point at 160M parameters. By allowing users to select an earlier exit point, MOSE provides a direct mechanism to decrease computational demands. This flexibility is crucial as smaller models generally require less energy and memory for inference, leading to more sustainable deployment options (Samsi et al., 2023).

We fine-tuned MOSE on SYNTHCONL (cf. Sec. 5 for details) for text-to-code and code-to-code retrieval, and on BIGCLONEBENCH (Svajlenko & Roy, 2015) for code clone detection, achieving state-of-the-art results among open models while maintaining deployment modularity.

Our contributions are as follows:

1. A self-distillation methodology that trains multiple model resolutions within a unified layer stack, reducing redundancy and improving scalability—an approach that could significantly impact LLM training pipelines dependent on multiple model distillations.
2. MOSE, pre-trained<sup>1</sup> and fine-tuned<sup>2</sup>, with up to 1 billion parameters and five exit points, allowing users to select model size based on memory and computational constraints.
3. SYNTHCONL<sup>3</sup>, a new dataset of 1,071,367 natural language-code-code triplets constructed via code translation, expanding text-to-code benchmarks with cross-language code-to-code pairs.

<sup>1</sup><https://huggingface.co/modularStarEncoder/ModularStarEncoder>

<sup>2</sup><https://huggingface.co/modularStarEncoder/ModularStarEncoder-finetuned>

<sup>3</sup><https://huggingface.co/datasets/modularStarEncoder/SynthCoNL>

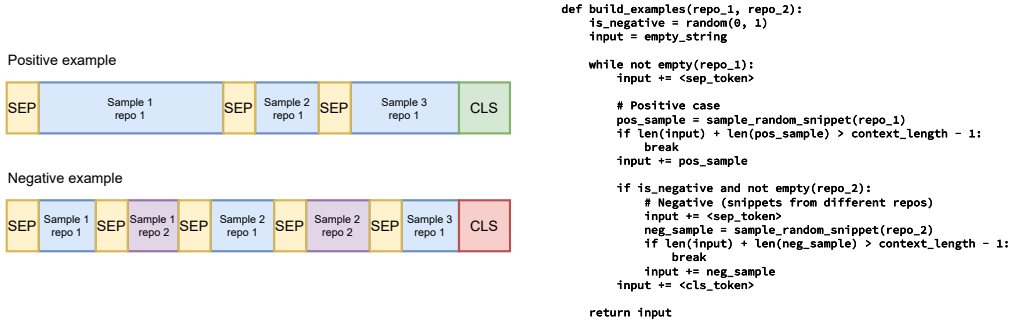


Figure 2: The illustration on the left depicts the in-context loss framework, where samples from various repositories are concatenated. Positive examples originate from the same repository context, whereas negative examples are sourced from different repositories. To enable the model’s use of FLASHATTENTION V2, we applied left padding and positioned the CLS token at the end of the sentence. On the right side, you’ll find the pseudocode for the in-context loss framework.

## 2 Self-Distillation and In-Context Classification

As different layers of transformer models capture varying degrees of semantic richness, often with intermediate layers proving most effective for specific tasks (Bolya et al., 2025), we design our pre-training strategy to support modularity and ease downstream task adaptability. Rather than treating the deepest layer as the sole source of meaningful representations, we aim to enhance representations throughout the network.

We hypothesize that *applying supervision at multiple depths*, not just at the output—encourages more robust and semantically rich intermediate representations. To this end, we combine multiple training objectives, each contributing to more versatile and generalizable embeddings (Wang et al., 2023). While we retain the widely adopted Masked Language Modeling (MLM) loss Feng et al. (2020), we discard the traditional Next Sentence Prediction (NSP) objective. NSP has been shown to offer minimal benefit after fine-tuning (Liu et al., 2019), and it imposes a rigid sentence-level structure that leads to inefficient use of context windows, especially for long-form code inputs. In its place, we introduce an In-Context Classification (ICC) loss (see section 2.1) that increases input density by reducing padding and fosters better chunk-level comprehension, essential for tasks like semantic retrieval or classification.

By integrating these two complementary objectives, MLM and ICC, and distributing their supervision across multiple layers, forming the basis of our *Self-Distillation* mechanism (see section 2.2), our training approach improves internal representation capabilities and flexibility, ultimately yielding a model better suited for modular deployment and early exiting.

### 2.1 Masked Language Modeling and In-Context Classification

We revisited the NSP loss and introduced an In-Context Classification (ICC) objective. We hypothesize that predicting whether multiple code snippets belong to the same context (in our case, the same repository) can enhance semantic search performance while allowing efficient concatenation of multiple code fragments. Our final training objective is the summation of two losses: (1) MLM loss and (2) ICC loss:  $\mathcal{L} = \mathcal{L}_{MLM} + \mathcal{L}_{ICC}$ .

In  $\mathcal{L}_{MLM}$ , a certain percentage of tokens are randomly masked and predicted using a classification head. Following Zhang et al. (2024), we adopt a 15% masking rate with the standard 80-10-10 token replacement strategy (Devlin et al., 2019). The secondary objective,  $\mathcal{L}_{ICC}$ , classifies whether randomly concatenated inputs (separated by a [SEP] special token) originate from the same repository (see fig. 2). Each concatenated sample has a 50% probability of containing source code from different repositories. This approach increases input density, reducing padding by expanding the average input length from 630 to 1,300 tokens. Since repositories are inherently modular and often contain files written in multiple languages, learning from repository-level context may also improve inter-language understanding.

Table 1: Performance—reported in MRR, and when specified in NDCG—of different models on text-to-code with CODESEARCHNET using CODEXGLUE. We reported the results presented in CODET5+, UNIXCODER and MODERNBERT (Wang et al., 2023; Guo et al., 2022; Warner et al., 2024). MOSE surpasses all existing open-source models, achieving an improvement of +3.6% compared to the best-performing open model, CODET5+. MOSE reduced the performance gap between open-source models and closed-source ones such as OPENAI TEXT-EMBEDDING-3-LARGE.

CodeSearchNet								
Model	Ruby	JS	Go	Python	Java	PHP	avg. MRR	avg. NDCG
MOSE	74.1	<b>74.0</b>	82.5	<b>92.5</b>	<b>78.7</b>	<b>84.5</b>	<b>81.0</b>	<b>84.2</b>
CODET5+ (770M)	<b>78.0</b>	71.3	<b>92.7</b>	75.8	76.2	70.1	77.4	-
UNIXCODER	74.0	68.4	91.5	72.0	72.6	67.6	74.4	-
MODERNBERT-LARGE	-	-	-	-	-	-	-	59.5
OPENAI TEXT-EMBEDDING-3-LARGE	84.7	85.3	95.9	99.8	90.1	95.6	91.9	93.3

## 2.2 Self-Distillation: Multi-Layer loss

To achieve layer-wise modularity in transformer architectures, we apply the previously introduced loss (section 2.1) across a selected set of layers, sharing classification heads (masked language modeling and in-context classification) *while incorporating a positional embedding of the layer index*. The total loss is computed as the sum of individual layer losses, weighted by a factor  $\alpha$  to prioritize deeper layers:  $\mathcal{L} = \sum_{i \in \iota} \mathcal{L}_i \cdot \alpha$  where  $\alpha = i/|I|$  and  $I = \{1, \dots, 36\}$  represents all layers, and the selected subset  $\iota = \{4, 9, 18, 27, 36\}$  defines the layers where the loss is applied. The selected subset was chosen to enable four model variants equally spaced in depth (9, 18, 27, 36) along with an additional “tiny” version (4) to see the model performance in a lower number of parameters set. This *Self-Distillation* mechanism, shown in Figure 1, allows for flexible model deployment, enabling adaptive layer pruning with minimal impact on performance.

## 3 Pre-training

We built MOSE on top of STARCODER-2 (Lozhkov et al., 2024), applying several modifications to the model. We reduced its original size, obtaining a model of 1B parameters. Our architecture comprises 36 hidden layers and adopts Grouped Query Attention (GQA) (Ainslie et al., 2023) with 16 attention heads and 4 key-value heads. MOSE relies upon Rotary Positional Encoding (RoPE) (Su et al., 2021) with a base period  $\theta = 10^{-6}$  and features a hidden dimensionality of 1,024 with an intermediate size of 12,288.

To make our model class bidirectional, we removed the causal masking from the self-attention operations within STARCODER-2. Aiming for modularity, we also replaced sliding window attention with full attention. This step was taken to avoid the receptive field phenomenon of the sliding window mechanisms (Zhu et al., 2021). Finally, our implementation integrates FLASHATTENTION V2 (Dao, 2023) for faster inference. We have included and summarized additional details about model architecture in appendix D.

### 3.1 Training Details

We pre-trained MOSE with a batch size of 4M tokens with a maximum context length of 2,048 tokens, for 245,000 training steps, processing approximately 1T tokens from THESTACKV2 (Lozhkov et al., 2024) dataset.

We used the AdamW optimizer with  $\beta_1$  set to 0.9,  $\beta_2$  to 0.95,  $\epsilon$  to  $1e-6$ , and a weight decay of  $1e-1$ . We initialized the learning rate at  $6.24e-4$  and decreased it using a multi-step learning rate scheduler (Bi et al., 2024) with 4,000 warmup steps. The learning rate was reduced at 120,000, 185,000, 220,000, 230,000, and 240,000 training steps, applying a decay factor of 0.36, and from step 185,000 onward, further reduced by factors of 0.1, 0.031, 0.01, and 0.001. We conducted pre-training and fine-tuning on 512 NVIDIA Ampere (64GB) GPUs, requiring 450,000 GPU working hours on the LEONARDO supercomputer (Turisini et al., 2023).

## 4 Downstream tasks

### 4.1 Finetuning for Retrieval, text-to-code and code-to-code search

Using the SYNTHCONL dataset detailed in section 5, we leveraged a instruction prompting approach Su et al. (2023) and trained a single model for both text-to-code and code-to-code retrieval tasks. The optimization objective uses CLIP loss (Radford et al., 2021) with the same multi-layer approach discussed in section 2.2, modified to enhance representation learning. Accordingly, we replaced the single-head projection of the multi-layer loss with five distinct projection heads, applied at different exit points of the pre-trained model (layers 4, 9, 18, 27, and 36). We used a batch of 2,048 elements, ensuring that text-to-code and code-to-code were equally distributed across the batch.

We performed data augmentation by randomly replacing frequently occurring words (appearing more than twice and having at least three characters) with random strings. We applied the augmentation exclusively to code snippets in 30% of cases, leaving natural language descriptions unchanged. After conducting a grid search, we selected  $1e-5$  as the learning rate, maintained throughout the finetuning process, and set the temperature parameter at 10.0.

### 4.2 Finetuning for classification, code clone detection

In addition to fine-tuning the model for multiple retrieval tasks as discussed in section 4.1, we also explored how our methodology performs in a classification setup. We tested how the Multi-Layer and the In-Context classification losses adapt to the code clone detection task by: (1) fine-tuning multiple classification heads — one for each of the five exit points (layers 4, 9, 18, 27, and 36), and (2) leveraging the model’s ability to understand relationships between code snippets by inputting pairs of (hypothetical clone) code segments and training it to classify whether they are clones. We followed the input pattern devised in section 2.1, formatting the input as follows: [SEP] *snippet-1* [SEP] *snippet-2* [CLS], and then used the final [CLS] token representation as input to a classifier. We fine-tuned the model with a constant learning rate of  $1e-5$  with 2,000 warmup steps, and used a batch size of 64 elements and trained for 14,000 steps.

Table 2: BIGCLONEBENCH code clone detection performance in a classification setup. MOSE maintains good performance (%) throughout different layers (L) with results on par with the state-of-the-art.

BigCloneBench			
Model	Recall	Precision	F1
MOSE (L4)	96.4	89.8	93.0
MOSE (L9)	<b>96.6</b>	90.4	93.4
MOSE (L18)	96.4	<b>92.1</b>	<b>94.2</b>
MOSE (L27)	96.5	91.8	94.1
MOSE (L36)	96.5	91.7	94.1
UNIXCODER	92.9	<b>97.6</b>	<b>95.2</b>
CODEBERT	94.7	93.4	94.1
CODET5+ (770M)	<b>96.7</b>	93.5	95.1

## 5 SYNTHCONL

We built SYNTHCONL, a dataset that supports training and evaluation of encoders in text-to-code and code-to-code search, under multiple languages. Using the popular CODESEARCHNET (Husain et al., 2019) as a seed dataset and selecting popular programming languages (Python, Java, Go, and PHP), we augmented it by transpiling available code snippets onto other languages.

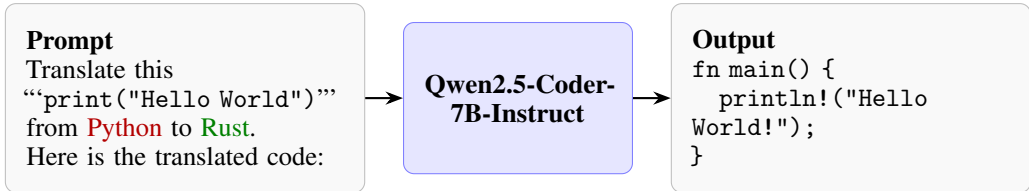


Figure 3: Prompt provided to QWEN2.5-CODER-7B-INSTRUCT for translating a given code snippet ( `print("Hello World")` in the example) from a source programming language (Python) to a target one (Rust).

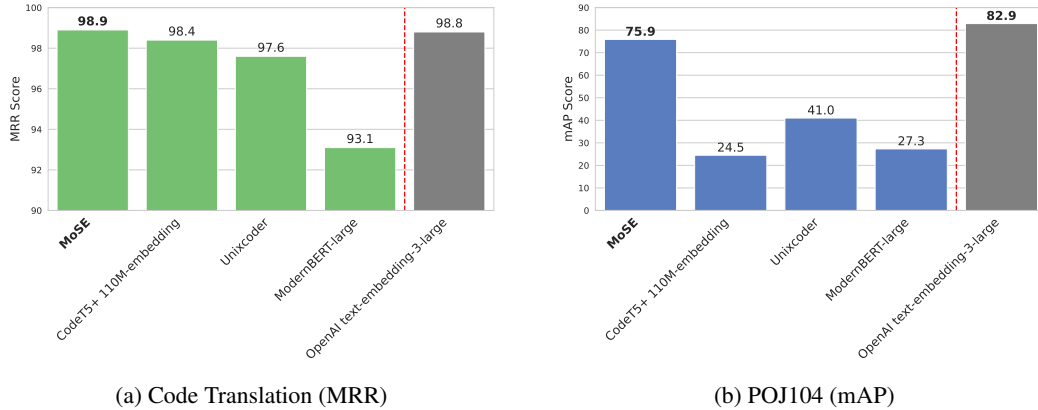


Figure 4: Performance of different models on CT and POJ104 for code-to-code retrieval with CODEXGLUE dataset. MOSE has state-of-the-art results with the CT benchmark and outperforms all the open-source models over the POJ104 benchmark. Compared to closed-source solutions (OPENAI TEXT-EMBEDDING-3-LARGE), MOSE performs on par in the code translation task and strongly reduces the gap between open- and closed-source models with the POJ104 benchmark.

To generate semantically similar code snippets for code-to-code search, we translated each snippet into a different language randomly sampled from Go, Ruby, Python, Java, C++, PHP, C, JavaScript. We prompted the QWEN2.5-CODER-7B-INSTRUCT model with the source code, the name of the source language, and the name of the target language (see fig. 3). During code translation, we carried out a greedy sampling so as to prevent semantic discrepancies.

This process yielded pairs of code snippets in distinct languages tied to the same natural language description. As a result, every sample in the fine-tuning dataset includes a natural language description and two code snippets from distinct languages. SYNTHCONL contains 1,071,367 triplets where, in the first code column, we directly sampled code snippets from CODESEARCHNET, including Python, Java, PHP, and Go. The second code column, artificially synthesized via code translation, includes Go, Ruby, JavaScript, Python, C++, PHP, C, and Java code snippets. After a manual inspection, we discovered that both columns contained code snippets that differed only in identifiers or function arguments. Several tasks were semantically identical but paraphrased with different parameter requirements (e.g., two identical paraphrased tasks asked for opening a socket on a different port). During the preprocessing phase of SYNTHCONL, motivated by the dataset’s redundancy and preliminary experiments that show its effectiveness on the model’s performance, we near-duplicated the dataset using both the CODESEARCHNET code column and the synthesized code column. During the data near deduplication phase, we relied on Locality Sensitive Hashing (LSH) with a Jaccard similarity threshold of 0.7 and 256 permutations, analyzing character-level 5-grams.

## 6 Results and Discussion

### 6.1 Evaluation

We evaluated MOSE, after fine-tuned for retrieval, on diverse code understanding tasks, leveraging the CODEXGLUE (Lu et al., 2021) group of benchmarks.

On CODESEARCHNET dataset, we assessed cross-modal (natural language to code) learning by retrieving target code from 999 distractors using natural language queries. For code-to-code retrieval, again against 999 distractors, we utilized CODEXGLUE’s Code Translation (CT) dataset to test cross-lingual retrieval (e.g., Java to C# snippets implementing the same functionality), and its POJ104 dataset (C++ snippets, semantically equivalent but syntactically different) for intra-lingual semantic search, evaluating generalization over structural differences while preserving semantics. In our retrieval performance evaluation, when comparing MOSE with other encoders, we included results from OPENAI’S TEXT-EMBEDDING-3-LARGE as a representative commercial, closed-source model.

Additionally, MOSE was fine-tuned and evaluated on the separate BIGCLONEBENCH (Svajlenko & Roy, 2015) dataset for Java code clone detection (a binary classification task), assessing its classification performance.

## 6.2 Benchmarks

Table 1 presents the results for the CODESEARCHNET (text-to-code) task in terms of Mean Reciprocal Rank (MRR, higher is better) for each single language, average Normalized Discounted Cumulative Gain (NDCG, higher is better), and average MRR. Results for UNIXCODER, MODERNBERT, and CODET5+ are reported from the original papers (Guo et al., 2022; Warner et al., 2024; Wang et al., 2023). On CODESEARCHNET, MOSE achieves an MRR of 81.0 and a NDCG of 84.2, outperforming CODET5+ (770M), UNIXCODER, and MODERNBERT-LARGE. The only encoder that surpasses MOSE is OPENAI’S TEXT-EMBEDDING-3-LARGE.

In Figure 4, we present results from both POJ104 and CT datasets reported respectively in terms of MRR for code translation (Java to C# retrieval) and mean average precision for POJ104 (C++ to C++ retrieval). MOSE reaches the best performance among the evaluated models. We further replicated the benchmarking for all models in a zero-shot setting for code-to-code tasks as our model does not integrate POJ104 and the code translation datasets in the training set. We present a comprehensive and detailed analysis of code retrieval errors in appendix C.

Referring to Figure 4, on the POJ104 dataset in zero-shot, MOSE achieves a mean Average Precision (mAP, higher is better) of 75.9, which is state-of-the-art among open-sourced models. However, it is significantly behind OPENAI TEXT-EMBEDDING-3-LARGE. We underscore that a direct comparison with OPENAI TEXT-EMBEDDING-3-LARGE remains challenging because it is closed-source, and details such as model size, training methodology, or potential data contamination are undisclosed.

We observe a marked difference in performance depending on whether the task is framed as text-to-code or code-to-code retrieval. As shown in Figure 1b, shallow layers yield better performance in the code-to-code setting, whereas for text-to-code retrieval, optimal performance emerges at layer 18.

This representation divergence suggests that the input modality influences where semantic alignment is most effectively captured within the model. This observation aligns with Valeriani et al. (2023) findings, underlining that *semantic information is distributed unevenly across layers* and is better expressed in the intermediate ones. MOSE leverages this property by supporting dynamic exit points, enabling users to balance computational cost and task performance based on where the most relevant representations emerge.

To further investigate this phenomenon, we compared similarity scores across layers to assess how each layer represents code snippets differently. Figure 5 shows permutation test results for a Python-to-Java retrieval task, highlighting significant variations in similarity scores that support our previous findings. A detailed analysis of these results is provided in appendix C.

In Table 2, we report classification performance across different exit layers of MOSE for the BIGCLONEBENCH benchmark. Results show stable performance throughout layers, with F1-scores from Layer 18 onward (94.2–94.1) closely matching those of deeper exits. Earlier layers (e.g., Layers 4 and 9) exhibit slightly lower precision, reflecting the expected trade-off between early inference and representational depth.

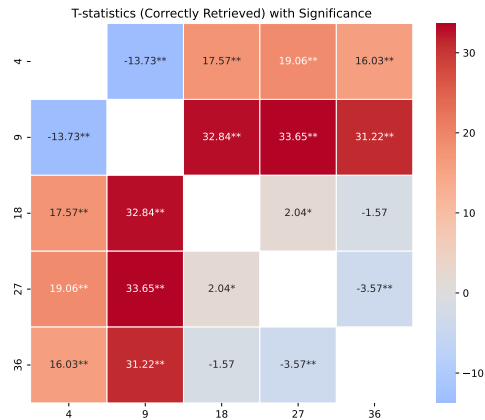


Figure 5: Similarity score Heatmap presenting results from permutation tests (10,000 permutations with  $\alpha = 0.05$ ) across different exit points for Python-to-Java retrieval. \* indicates  $p < 0.05$  and \*\* indicates  $p < 0.001$ . Different layers, despite a common training objective, yield different similarity scores.

Table 3: Performance comparison of MOSE layers and baseline fine-tuned models on the CODESEARCHNET benchmark. The table displays the overall retrieval performance measured by the Mean Reciprocal Rank (MRR, higher is better). We refer to MOSE, fine-tuned with multiple exit points simultaneously, as *Self-Distilled*. The models not marked as self-distilled are the baselines, fine-tuned individually for each exit point. MOSE fine-tuned with multi-layer loss (Self-Distillation) consistently outperforms the baselines, showing a more significant difference in the initial layers.

CodeSearchNet									
Model type	Num. Layers	Num. Params.	Ruby	Javascript	Go	Python	Java	PHP	avg. MRR
<i>Base</i>	4	160M	59.5	61.3	72.1	86.2	68.2	75.5	70.5
<i>Self-Distilled</i>			<b>62.2</b>	<b>64.7</b>	<b>74.8</b>	<b>88.1</b>	<b>71.4</b>	<b>78.0</b>	<b>73.2</b>
<i>Base</i>	9	300M	64.9	65.7	74.3	87.3	72.0	78.8	73.8
<i>Self-Distilled</i>			<b>67.6</b>	<b>69.4</b>	<b>78.9</b>	<b>90.2</b>	<b>75.5</b>	<b>82.3</b>	<b>77.3</b>
<i>Base</i>	18	550M	73.8	73.5	82.4	92.1	78.4	84.0	80.7
<i>Self-Distilled</i>			<b>74.1</b>	<b>74.0</b>	<b>82.5</b>	<b>92.5</b>	<b>78.7</b>	<b>84.5</b>	<b>81.0</b>
<i>Base</i>	27	800M	72.3	71.8	80.8	90.8	76.9	82.3	79.1
<i>Self-Distilled</i>			<b>73.2</b>	<b>73.3</b>	<b>81.7</b>	<b>92.1</b>	<b>77.8</b>	<b>83.8</b>	<b>80.3</b>
<i>Base</i>	36	1B	72.3	72.9	80.7	91.5	77.1	82.9	79.5
<i>Self-Distilled</i>			<b>73.5</b>	72.6	80.5	91.4	76.9	82.7	<b>79.6</b>

Our method remains competitive compared to state-of-the-art models. While CODET5+ (770M) and UNIXCODER achieve peaks F1 of 95.1 and 95.2, MOSE delivers on-par results (-0.9) by Layer 18, with the added benefit of a modular architecture.

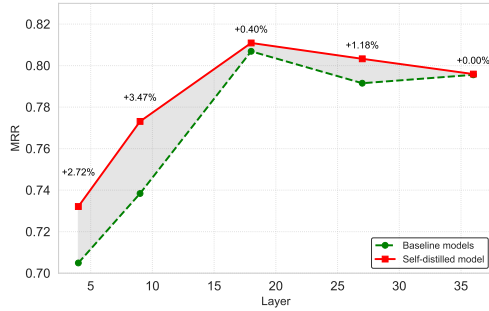
### 6.3 Ablation Study

We conducted an ablation study for the Multi-Layer loss, by fine-tuning (starting from MOSE, pre-trained) on SYNTHCONL, each exit point singularly (e.g., for the baseline on layer 18, we retain only the first 18 layers and fine-tune the model using just the projection head on that layer). Finally, we compared the baseline models with the corresponding results (Self-Distilled) of MOSE fine-tuned for retrieval with the multi-layer loss; all tests are conducted on the CODESEARCHNET dataset. MOSE consistently outperforms the single-exit baselines (up to +4.36% averaged Recall@1 gain on layer 9), indicating that *lower-level layers benefit from training signals propagated from deeper layers*. This behavior is highlighted in Table 3, where MOSE, indicated as *Self-Distilled*, outperforms all the single exit baselines consistently. This finding underscores a promising new direction in Self-Distillation for large-scale code and text models, enabling high performance even in more compact configurations. Moreover, Figure 6 illustrates that MOSE maintains robust performance from layers 18 to 36, allowing users to scale down the network to match their memory, computational, or latency constraints while preserving strong retrieval performances.

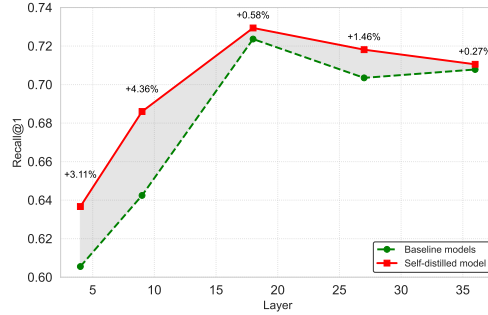
## 7 Related work

Since the introduction of ELMo (Peters et al., 2018), deep contextual information has enhanced generating embeddings for textual retrieval or classification, reaching state-of-the-art results in several tasks. BERT (Feng et al., 2020) followed those findings, adapting the Transformer architecture (Vaswani et al., 2017) to enable a bi-directional representation with two different training objectives, namely the masked language modeling and the next sentence prediction losses. Lan et al. (2019) and Liu et al. (2019) adapted the BERT architecture to obtain an enhanced pre-trained model by removing or modifying the NSP, focusing on pre-training data or hyperparameters optimization. More recently, MODERNBERT (Warner et al., 2024) tied the gap between modern decoders (Jiang et al., 2023; Hui et al., 2024; Dubey et al., 2024; Touvron et al., 2023; Lozhkov et al., 2024) advancements that rely upon models with an increased number of parameters, trained upon more tokens, and being capable of handling longer contextual information.

In code representation, large language models must be adapted by training them on a curated corpus focused on software and by leveraging code’s syntactic and semantic structures, which differ significantly from natural language. Feng et al. (2020) adapted the BERT architecture to



(a) MRR × Embedding depth



(b) Recall@1 × Embedding depth

Figure 6: Performance Comparison between MOSE fine-tuned with Multi-layer loss (Self-Distilled model) and baselines fine-tuned just on single exit points: The graph illustrates averaged MRR and Recall@1 results for different layers over the CODESEARCHNET test set. Layers fine-tuned with Multi-Layer loss outperforms the baselines (up to 3.47% MRR and +4.36% Recall@1).

produce semantically meaningful embeddings for source code, resulting in CODEBERT. This was accomplished by including more source code in the training set and focusing on a training loss that can leverage bimodal (natural language and code) contextual information (Clark et al., 2020). GRAPHCODEBERT enhanced CODEBERT (Feng et al., 2020) representations by incorporating data flow graphs, capturing dependencies between variables and operations, and improving tasks like code summarization and clone detection. UNIXCODER (Guo et al., 2022) extended this by introducing a unified encoder-decoder framework, integrating abstract syntax trees (ASTs) and data flow information. Wang et al. (2023) expanded these findings with CODET5+, stressing how multiple losses that leverage code semantics impact the model pertaining. The work incorporated text-code contrastive learning, text-code Matching, and text-code causal LM for better code understanding and generation.

When trying to achieve better performance, research has shifted toward models with a high number of parameters. While this trend appears effective from a performance perspective, end users may face computational or memory limitations as LLMs vary from millions to billions of parameters. Sanh et al. (2019) pioneered the introduction of knowledge distillation, using a “teacher” model that guides a smaller model to emulate its behavior. This methodology has been widely adopted and improved upon recently (DeepSeek-AI et al., 2025; Hui et al., 2024), becoming a standard for obtaining high-performing smaller LLMs.

Our work differs from previous work by adapting a modern architecture (STARCODER-2 (Lozhkov et al., 2024)) to a code encoder-only based model and introducing a novel ‘Self-Distillation’ mechanism. We replace the next sentence prediction loss with an In-Context Classification focused on the repository level and expand the context to 2,048 tokens. Our novel Self-Distillation mechanism improves low-level layers, resulting in a modular transformer architecture without additional teacher models or further data for distillation.

## 8 Conclusion

We introduced MOSE, a modular, multi-exit encoder that uses Self-Distillation to enhance early-layer representations while achieving state-of-the-art results on code understanding benchmarks. By integrating multiple exit points, MOSE enables explicit efficiency-accuracy trade-offs tailored to deployment constraints. Our approach not only allows for modular use but also enhances the alignment between task requirements and representation depth. This improves task-specific layer specialization, providing the end-user with a more adaptable model.

Future work will explore combining exit-points and further understanding task type and depth interactions. While our results are encouraging, we acknowledge that computational constraints limited extensive hyperparameter tuning and pre-training ablations, and that fine-tuning with synthetic code generated from code translation has an unclear impact. We discuss these limitations in detail in appendix A.

## Acknowledgments

We acknowledge ISCRA for awarding this project access to the LEONARDO supercomputer, owned by the EuroHPC Joint Undertaking, hosted by CINECA (Italy).

This work was supported by Future AI Research (FAIR) PE01, SPOKE 8 on PERVASIVE AI funded by the National Recovery and Resilience Plan (NRRP).

## References

- Joshua Ainslie, James Lee-Thorp, Michiel de Jong, Yury Zemlyanskiy, Federico Lebrón, and Sumit Sanghai. GQA: Training Generalized Multi-Query Transformer Models from Multi-Head Checkpoints. *arXiv e-prints*, art. arXiv:2305.13245, May 2023. doi: 10.48550/arXiv.2305.13245.
- Loubna Ben Allal, Anton Lozhkov, Elie Bakouch, Gabriel Martín Blázquez, Guilherme Penedo, Lewis Tunstall, Andrés Marafioti, Hynek Kydlíček, Agustín Piqueres Lajarín, Vaibhav Srivastav, et al. Smollm2: When smol goes big—data-centric training of a small language model. *arXiv preprint arXiv:2502.02737*, 2025.
- Xiao Bi, Deli Chen, Guanting Chen, Shanhuang Chen, Damai Dai, Chengqi Deng, Honghui Ding, Kai Dong, Qiusi Du, Zhe Fu, Huazuo Gao, Kaige Gao, Wenjun Gao, Ruiqi Ge, Kang Guan, Daya Guo, Jianzhong Guo, Guangbo Hao, Zhewen Hao, Ying He, Wenjie Hu, Panpan Huang, Erhang Li, Guowei Li, Jiashi Li, Yao Li, Y. K. Li, Wenfeng Liang, Fangyun Lin, Alex X. Liu, Bo Liu, Wen Liu, Xiaodong Liu, Xin Liu, Yiyuan Liu, Haoyu Lu, Shanghao Lu, Fuli Luo, Shirong Ma, Xiaotao Nie, Tian Pei, Yishi Piao, Junjie Qiu, Hui Qu, Tongzheng Ren, Zehui Ren, Chong Ruan, Zhangli Sha, Zhihong Shao, Junxiao Song, Xuecheng Su, Jingxiang Sun, Yaofeng Sun, Minghui Tang, Bingxuan Wang, Peiyi Wang, Shiyu Wang, Yaohui Wang, Yongji Wang, Tong Wu, Y. Wu, Xin Xie, Zhenda Xie, Ziwei Xie, Yiliang Xiong, Hanwei Xu, R. X. Xu, Yanhong Xu, Dejian Yang, Yuxiang You, Shuiping Yu, Xingkai Yu, B. Zhang, Haowei Zhang, Lecong Zhang, Liyue Zhang, Mingchuan Zhang, Minghua Zhang, Wentao Zhang, Yichao Zhang, Chenggang Zhao, Yao Zhao, Shangyan Zhou, Shunfeng Zhou, Qihao Zhu, and Yuheng Zou. Deepseek LLM: scaling open-source language models with longtermism. *CoRR*, abs/2401.02954, 2024. doi: 10.48550/ARXIV.2401.02954. URL <https://doi.org/10.48550/arXiv.2401.02954>.
- Daniel Bolya, Po-Yao Huang, Peize Sun, Jang Hyun Cho, Andrea Madotto, Chen Wei, Tengyu Ma, Jiale Zhi, Jathushan Rajasegaran, Hanoona Rasheed, Junke Wang, Marco Monteiro, Hu Xu, Shiyu Dong, Nikhila Ravi, Daniel Li, Piotr Dollár, and Christoph Feichtenhofer. Perception encoder: The best visual embeddings are not at the output of the network, 2025. URL <https://arxiv.org/abs/2504.13181>.
- Ting Chen, Simon Kornblith, Mohammad Norouzi, and Geoffrey E. Hinton. A simple framework for contrastive learning of visual representations. In *Proceedings of the 37th International Conference on Machine Learning, ICML 2020, 13-18 July 2020, Virtual Event*, volume 119 of *Proceedings of Machine Learning Research*, pp. 1597–1607. PMLR, 2020. URL <http://proceedings.mlr.press/v119/chen20j.html>.
- Kevin Clark, Minh-Thang Luong, Quoc V. Le, and Christopher D. Manning. ELECTRA: pre-training text encoders as discriminators rather than generators. In *8th International Conference on Learning Representations, ICLR 2020, Addis Ababa, Ethiopia, April 26-30, 2020*. OpenReview.net, 2020. URL <https://openreview.net/forum?id=r1xMH1BtvB>.
- Tri Dao. FlashAttention-2: Faster Attention with Better Parallelism and Work Partitioning. *arXiv e-prints*, art. arXiv:2307.08691, July 2023. doi: 10.48550/arXiv.2307.08691.
- DeepSeek-AI, Daya Guo, Dejian Yang, Haowei Zhang, Junxiao Song, Ruoyu Zhang, Runxin Xu, Qihao Zhu, Shirong Ma, Peiyi Wang, Xiao Bi, Xiaokang Zhang, Xingkai Yu, Yu Wu, Z. F. Wu, Zhibin Gou, Zhihong Shao, Zhuoshu Li, Ziyi Gao, Aixin Liu, Bing Xue, Bingxuan Wang, Bochao Wu, Bei Feng, Chengda Lu, Chenggang Zhao, Chengqi Deng, Chenyu Zhang, Chong Ruan, Damai Dai, Deli Chen, Dongjie Ji, Erhang Li, Fangyun Lin, Fucong Dai, Fuli Luo, Guangbo Hao, Guanting Chen, Guowei Li, H. Zhang, Han Bao, Hanwei Xu, Haocheng Wang, Honghui Ding, Huajian Xin, Huazuo Gao, Hui Qu, Hui Li, Jianzhong Guo, Jiashi Li, Jiawei Wang, Jingchang

- Chen, Jingyang Yuan, Junjie Qiu, Junlong Li, J. L. Cai, Jiaqi Ni, Jian Liang, Jin Chen, Kai Dong, Kai Hu, Kaige Gao, Kang Guan, Kexin Huang, Kuai Yu, Lean Wang, Lecong Zhang, Liang Zhao, Litong Wang, Liyue Zhang, Lei Xu, Leyi Xia, Mingchuan Zhang, Minghua Zhang, Minghui Tang, Meng Li, Miaojun Wang, Mingming Li, Ning Tian, Panpan Huang, Peng Zhang, Qiancheng Wang, Qinyu Chen, Qiushi Du, Ruiqi Ge, Ruisong Zhang, Ruizhe Pan, Runji Wang, R. J. Chen, R. L. Jin, Ruyi Chen, Shanghao Lu, Shangyan Zhou, Shanhuang Chen, Shengfeng Ye, Shiyu Wang, Shuiping Yu, Shunfeng Zhou, Shuting Pan, S. S. Li, Shuang Zhou, Shaoqing Wu, Shengfeng Ye, Tao Yun, Tian Pei, Tianyu Sun, T. Wang, Wangding Zeng, Wanxia Zhao, Wen Liu, Wenfeng Liang, Wenjun Gao, Wenqin Yu, Wentao Zhang, W. L. Xiao, Wei An, Xiaodong Liu, Xiaohan Wang, Xiaokang Chen, Xiaotao Nie, Xin Cheng, Xin Liu, Xin Xie, Xingchao Liu, Xinyu Yang, Xinyuan Li, Xuecheng Su, Xuheng Lin, X. Q. Li, Xiangyue Jin, Xiaojin Shen, Xiaosha Chen, Xiaowen Sun, Xiaoxiang Wang, Xinnan Song, Xinyi Zhou, Xianzu Wang, Xinxia Shan, Y. K. Li, Y. Q. Wang, Y. X. Wei, Yang Zhang, Yanhong Xu, Yao Li, Yao Zhao, Yaofeng Sun, Yaohui Wang, Yi Yu, Yichao Zhang, Yifan Shi, Yiliang Xiong, Ying He, Yishi Piao, Yisong Wang, Yixuan Tan, Yiyang Ma, Yiyuan Liu, Yongqiang Guo, Yuan Ou, Yudian Wang, Yue Gong, Yuheng Zou, Yujia He, Yunfan Xiong, Yuxiang Luo, Yuxiang You, Yuxuan Liu, Yuyang Zhou, Y. X. Zhu, Yanhong Xu, Yanping Huang, Yaohui Li, Yi Zheng, Yuchen Zhu, Yunxian Ma, Ying Tang, Yukun Zha, Yuting Yan, Z. Z. Ren, Zehui Ren, Zhangli Sha, Zhe Fu, Zhean Xu, Zhenda Xie, Zhengyan Zhang, Zhewen Hao, Zhicheng Ma, Zhigang Yan, Zhiyu Wu, Zihui Gu, Zijia Zhu, Zijun Liu, Zilin Li, Ziwei Xie, Ziyang Song, Zizheng Pan, Zhen Huang, Zhipeng Xu, Zhongyu Zhang, and Zhen Zhang. Deepseek-r1: Incentivizing reasoning capability in llms via reinforcement learning, 2025. URL <https://arxiv.org/abs/2501.12948>.
- Jacob Devlin, Ming-Wei Chang, Kenton Lee, and Kristina Toutanova. BERT: pre-training of deep bidirectional transformers for language understanding. In Jill Burstein, Christy Doran, and Thamar Solorio (eds.), *Proceedings of the 2019 Conference of the North American Chapter of the Association for Computational Linguistics: Human Language Technologies, NAACL-HLT 2019, Minneapolis, MN, USA, June 2-7, 2019, Volume 1 (Long and Short Papers)*, pp. 4171–4186. Association for Computational Linguistics, 2019. doi: 10.18653/V1/N19-1423. URL <https://doi.org/10.18653/v1/n19-1423>.
- Abhimanyu Dubey, Abhinav Jauhri, Abhinav Pandey, Abhishek Kadian, Ahmad Al-Dahle, Aiesha Letman, Akhil Mathur, Alan Schelten, Amy Yang, Angela Fan, Anirudh Goyal, Anthony Hartshorn, Aobo Yang, Archi Mitra, Archie Sravankumar, Artem Korenev, Arthur Hinsvark, Arun Rao, Aston Zhang, Aurélien Rodriguez, Austen Gregerson, Ava Spataru, Baptiste Rozière, Bethany Biron, Binh Tang, Bobbie Chern, Charlotte Caucheteux, Chaya Nayak, Chloe Bi, Chris Marra, Chris McConnell, Christian Keller, Christophe Touret, Chunyang Wu, Corinne Wong, Cristian Canton Ferrer, Cyrus Nikolaidis, Damien Allonsius, Daniel Song, Danielle Pintz, Danny Livshits, David Esiobu, Dhruv Choudhary, Dhruv Mahajan, Diego Garcia-Olano, Diego Perino, Dieuwke Hupkes, Egor Lakomkin, Ehab AlBadawy, Elina Lobanova, Emily Dinan, Eric Michael Smith, Filip Radenovic, Frank Zhang, Gabriel Synnaeve, Gabrielle Lee, Georgia Lewis Anderson, Graeme Nail, Grégoire Mialon, Guan Pang, Guillem Cucurell, Hailey Nguyen, Hannah Korevaar, Hu Xu, Hugo Touvron, Iliyan Zarov, Imanol Arrieta Ibarra, Isabel M. Kloumann, Ishan Misra, Ivan Evtimov, Jade Copet, Jaewon Lee, Jan Geffert, Jana Vranes, Jason Park, Jay Mahadeokar, Jeet Shah, Jelmer van der Linde, Jennifer Billock, Jenny Hong, Jenya Lee, Jeremy Fu, Jianfeng Chi, Jianyu Huang, Jiawen Liu, Jie Wang, Jiecao Yu, Joanna Bitton, Joe Spisak, Jongsoo Park, Joseph Rocca, Joshua Johnstun, Joshua Saxe, Junteng Jia, Kalyan Vasuden Alwala, Kartikeya Upasani, Kate Plawiak, Ke Li, Kenneth Heafield, Kevin Stone, and et al. The llama 3 herd of models. *CoRR*, abs/2407.21783, 2024. doi: 10.48550/ARXIV.2407.21783. URL <https://doi.org/10.48550/arXiv.2407.21783>.
- Vage Egiazarian, Andrei Panferov, Denis Kuznedelev, Elias Frantar, Artem Babenko, and Dan Alistarh. Extreme Compression of Large Language Models via Additive Quantization. *arXiv e-prints*, art. arXiv:2401.06118, January 2024. doi: 10.48550/arXiv.2401.06118.
- Zhangyin Feng, Daya Guo, Duyu Tang, Nan Duan, Xiaocheng Feng, Ming Gong, Linjun Shou, Bing Qin, Ting Liu, Daxin Jiang, and Ming Zhou. CodeBERT: A Pre-Trained Model for Programming and Natural Languages. *arXiv e-prints*, art. arXiv:2002.08155, February 2020. doi: 10.48550/arXiv.2002.08155.
- Zhangyin Feng, Daya Guo, Duyu Tang, Nan Duan, Xiaocheng Feng, Ming Gong, Linjun Shou, Bing Qin, Ting Liu, Daxin Jiang, and Ming Zhou. Codebert: A pre-trained model for programming and

- natural languages. In Trevor Cohn, Yulan He, and Yang Liu (eds.), *Findings of the Association for Computational Linguistics: EMNLP 2020, Online Event, 16-20 November 2020*, volume EMNLP 2020 of *Findings of ACL*, pp. 1536–1547. Association for Computational Linguistics, 2020. doi: 10.18653/V1/2020.FINDINGS-EMNLP.139. URL <https://doi.org/10.18653/v1/2020.findings-emnlp.139>.
- Daya Guo, Shuai Lu, Nan Duan, Yanlin Wang, Ming Zhou, and Jian Yin. Unixcoder: Unified cross-modal pre-training for code representation. In Smaranda Muresan, Preslav Nakov, and Aline Villavicencio (eds.), *Proceedings of the 60th Annual Meeting of the Association for Computational Linguistics (Volume 1: Long Papers), ACL 2022, Dublin, Ireland, May 22-27, 2022*, pp. 7212–7225. Association for Computational Linguistics, 2022. doi: 10.18653/V1/2022.ACL-LONG.499. URL <https://doi.org/10.18653/v1/2022.acl-long.499>.
- Song Han, Jeff Pool, John Tran, and William J. Dally. Learning both Weights and Connections for Efficient Neural Networks. *arXiv e-prints*, art. arXiv:1506.02626, June 2015. doi: 10.48550/arXiv.1506.02626.
- Binyuan Hui, Jian Yang, Zeyu Cui, Jiayi Yang, Dayiheng Liu, Lei Zhang, Tianyu Liu, Jiajun Zhang, Bowen Yu, Kai Dang, An Yang, Rui Men, Fei Huang, Xingzhang Ren, Xuancheng Ren, Jingren Zhou, and Junyang Lin. Qwen2.5-coder technical report. *CoRR*, abs/2409.12186, 2024. doi: 10.48550/ARXIV.2409.12186. URL <https://doi.org/10.48550/arXiv.2409.12186>.
- Hamel Husain, Ho-Hsiang Wu, Tiferet Gazit, Miltiadis Allamanis, and Marc Brockschmidt. Code-searchnet challenge: Evaluating the state of semantic code search. *CoRR*, abs/1909.09436, 2019. URL <http://arxiv.org/abs/1909.09436>.
- Benoit Jacob, Skirmantas Kligys, Bo Chen, Menglong Zhu, Matthew Tang, Andrew Howard, Hartwig Adam, and Dmitry Kalenichenko. Quantization and Training of Neural Networks for Efficient Integer-Arithmetic-Only Inference. *arXiv e-prints*, art. arXiv:1712.05877, December 2017. doi: 10.48550/arXiv.1712.05877.
- Albert Q. Jiang, Alexandre Sablayrolles, Arthur Mensch, Chris Bamford, Devendra Singh Chaplot, Diego de las Casas, Florian Bressand, Gianna Lengyel, Guillaume Lample, Lucile Saulnier, L lio Renard Lavaud, Marie-Anne Lachaux, Pierre Stock, Teven Le Scao, Thibaut Lavril, Thomas Wang, Timoth e Lacroix, and William El Sayed. Mistral 7B. *arXiv e-prints*, art. arXiv:2310.06825, October 2023. doi: 10.48550/arXiv.2310.06825.
- Xiaoqi Jiao, Yichun Yin, Lifeng Shang, Xin Jiang, Xiao Chen, Linlin Li, Fang Wang, and Qun Liu. TinyBERT: Distilling BERT for Natural Language Understanding. *arXiv e-prints*, art. arXiv:1909.10351, September 2019. doi: 10.48550/arXiv.1909.10351.
- Aditya Kusupati, Gantavya Bhatt, Aniket Rege, Matthew Wallingford, Aditya Sinha, Vivek Ramanujan, William Howard-Snyder, Kaifeng Chen, Sham Kakade, Prateek Jain, and Ali Farhadi. Matryoshka representation learning. In S. Koyejo, S. Mohamed, A. Agarwal, D. Belgrave, K. Cho, and A. Oh (eds.), *Advances in Neural Information Processing Systems*, volume 35, pp. 30233–30249. Curran Associates, Inc., 2022. URL [https://proceedings.neurips.cc/paper\\_files/paper/2022/file/c32319f4868da7613d78af9993100e42-Paper-Conference.pdf](https://proceedings.neurips.cc/paper_files/paper/2022/file/c32319f4868da7613d78af9993100e42-Paper-Conference.pdf).
- Zhenzhong Lan, Mingda Chen, Sebastian Goodman, Kevin Gimpel, Piyush Sharma, and Radu Soricut. ALBERT: A Lite BERT for Self-supervised Learning of Language Representations. *arXiv e-prints*, art. arXiv:1909.11942, September 2019. doi: 10.48550/arXiv.1909.11942.
- Ji Lin, Jiaming Tang, Haotian Tang, Shang Yang, Wei-Ming Chen, Wei-Chen Wang, Guangxuan Xiao, Xingyu Dang, Chuang Gan, and Song Han. AWQ: Activation-aware Weight Quantization for LLM Compression and Acceleration. *arXiv e-prints*, art. arXiv:2306.00978, June 2023. doi: 10.48550/arXiv.2306.00978.
- Yinhan Liu, Myle Ott, Naman Goyal, Jingfei Du, Mandar Joshi, Danqi Chen, Omer Levy, Mike Lewis, Luke Zettlemoyer, and Veselin Stoyanov. Roberta: A robustly optimized BERT pretraining approach. *CoRR*, abs/1907.11692, 2019. URL <http://arxiv.org/abs/1907.11692>.

- Anton Lozhkov, Raymond Li, Loubna Ben Allal, Federico Cassano, Joel Lamy-Poirier, Nouamane Tazi, Ao Tang, Dmytro Pykhtar, Jiawei Liu, Yuxiang Wei, Tianyang Liu, Max Tian, Denis Kocetkov, Arthur Zucker, Younes Belkada, Zijian Wang, Qian Liu, Dmitry Abulkhanov, Indraneil Paul, Zhuang Li, Wen-Ding Li, Megan Risdal, Jia Li, Jian Zhu, Terry Yue Zhuo, Evgenii Zheltonozhskii, Nii Osaе Osaе Dade, Wenhao Yu, Lucas Krauß, Naman Jain, Yixuan Su, Xuanli He, Manan Dey, Edoardo Abati, Yekun Chai, Niklas Muennighoff, Xiangru Tang, Muhtasham Oblokulov, Christopher Akiki, Marc Marone, Chenghao Mou, Mayank Mishra, Alex Gu, Binyuan Hui, Tri Dao, Armel Zebaze, Olivier Dehaene, Nicolas Patry, Canwen Xu, Julian McAuley, Han Hu, Torsten Scholak, Sebastien Paquet, Jennifer Robinson, Carolyn Jane Anderson, Nicolas Chapados, Mostofa Patwary, Nima Tajbakhsh, Yacine Jernite, Carlos Muñoz Ferrandis, Lingming Zhang, Sean Hughes, Thomas Wolf, Arjun Guha, Leandro von Werra, and Harm de Vries. StarCoder 2 and The Stack v2: The Next Generation. *arXiv e-prints*, art. arXiv:2402.19173, February 2024. doi: 10.48550/arXiv.2402.19173.
- Shuai Lu, Daya Guo, Shuo Ren, Junjie Huang, Alexey Svyatkovskiy, Ambrosio Blanco, Colin B. Clement, Dawn Drain, Daxin Jiang, Duyu Tang, Ge Li, Lidong Zhou, Linjun Shou, Long Zhou, Michele Tufano, Ming Gong, Ming Zhou, Nan Duan, Neel Sundaresan, Shao Kun Deng, Shengyu Fu, and Shujie Liu. Codexglue: A machine learning benchmark dataset for code understanding and generation. In Joaquin Vanschoren and Sai-Kit Yeung (eds.), *Proceedings of the Neural Information Processing Systems Track on Datasets and Benchmarks 1, NeurIPS Datasets and Benchmarks 2021, December 2021, virtual*, 2021. URL <https://datasets-benchmarks-proceedings.neurips.cc/paper/2021/hash/c16a5320fa475530d9583c34fd356ef5-Abstract-round1.html>.
- Changan Niu, Chuanyi Li, Vincent Ng, Dongxiao Chen, Jidong Ge, and Bin Luo. An empirical comparison of pre-trained models of source code. In *2023 IEEE/ACM 45th International Conference on Software Engineering (ICSE)*, pp. 2136–2148. IEEE, 2023.
- Matthew E. Peters, Mark Neumann, Mohit Iyyer, Matt Gardner, Christopher Clark, Kenton Lee, and Luke Zettlemoyer. Deep contextualized word representations. In Marilyn Walker, Heng Ji, and Amanda Stent (eds.), *Proceedings of the 2018 Conference of the North American Chapter of the Association for Computational Linguistics: Human Language Technologies, Volume 1 (Long Papers)*, pp. 2227–2237, New Orleans, Louisiana, June 2018. Association for Computational Linguistics. doi: 10.18653/v1/N18-1202. URL <https://aclanthology.org/N18-1202/>.
- Alec Radford, Jong Wook Kim, Chris Hallacy, Aditya Ramesh, Gabriel Goh, Sandhini Agarwal, Girish Sastry, Amanda Askell, Pamela Mishkin, Jack Clark, Gretchen Krueger, and Ilya Sutskever. Learning transferable visual models from natural language supervision. In Marina Meila and Tong Zhang (eds.), *Proceedings of the 38th International Conference on Machine Learning, ICML 2021, 18-24 July 2021, Virtual Event*, volume 139 of *Proceedings of Machine Learning Research*, pp. 8748–8763. PMLR, 2021. URL <http://proceedings.mlr.press/v139/radford21a.html>.
- Siddharth Samsi, Dan Zhao, Joseph McDonald, Baolin Li, Adam Michaleas, Michael Jones, William Bergeron, Jeremy Kepner, Devesh Tiwari, and Vijay Gadepally. From words to watts: Benchmarking the energy costs of large language model inference. In *IEEE High Performance Extreme Computing Conference, HPEC 2023, Boston, MA, USA, September 25-29, 2023*, pp. 1–9. IEEE, 2023. doi: 10.1109/HPEC58863.2023.10363447. URL <https://doi.org/10.1109/HPEC58863.2023.10363447>.
- Victor Sanh, Lysandre Debut, Julien Chaumond, and Thomas Wolf. DistilBERT, a distilled version of BERT: smaller, faster, cheaper and lighter. *arXiv e-prints*, art. arXiv:1910.01108, October 2019. doi: 10.48550/arXiv.1910.01108.
- Hongjin Su, Weijia Shi, Jungo Kasai, Yizhong Wang, Yushi Hu, Mari Ostendorf, Wen-tau Yih, Noah A. Smith, Luke Zettlemoyer, and Tao Yu. One embedder, any task: Instruction-finetuned text embeddings. In Anna Rogers, Jordan L. Boyd-Graber, and Naoaki Okazaki (eds.), *Findings of the Association for Computational Linguistics: ACL 2023, Toronto, Canada, July 9-14, 2023*, pp. 1102–1121. Association for Computational Linguistics, 2023. doi: 10.18653/v1/2023.FINDINGS-ACL.71. URL <https://doi.org/10.18653/v1/2023.findings-acl.71>.

- Jianlin Su, Yu Lu, Shengfeng Pan, Ahmed Murtadha, Bo Wen, and Yunfeng Liu. RoFormer: Enhanced Transformer with Rotary Position Embedding. *arXiv e-prints*, art. arXiv:2104.09864, April 2021. doi: 10.48550/arXiv.2104.09864.
- Jeffrey Svajlenko and Chanchal K. Roy. Evaluating clone detection tools with bigclonebench. In *2015 IEEE International Conference on Software Maintenance and Evolution (ICSME)*, pp. 131–140, 2015. doi: 10.1109/ICSM.2015.7332459.
- Surat Teerapittayanon, Bradley McDanel, and H. T. Kung. BranchyNet: Fast Inference via Early Exiting from Deep Neural Networks. *arXiv e-prints*, art. arXiv:1709.01686, September 2017. doi: 10.48550/arXiv.1709.01686.
- Hugo Touvron, Louis Martin, Kevin Stone, Peter Albert, Amjad Almahairi, Yasmine Babaei, Nikolay Bashlykov, Soumya Batra, Prajwal Bhargava, Shruti Bhosale, Dan Bikel, Lukas Blecher, Cristian Canton-Ferrer, Moya Chen, Guillem Cucurull, David Esiobu, Jude Fernandes, Jeremy Fu, Wenyin Fu, Brian Fuller, Cynthia Gao, Vedanuj Goswami, Naman Goyal, Anthony Hartshorn, Saghar Hosseini, Rui Hou, Hakan Inan, Marcin Kardas, Viktor Kerkez, Madian Khabsa, Isabel Kloumann, Artem Korenev, Punit Singh Koura, Marie-Anne Lachaux, Thibaut Lavril, Jenya Lee, Diana Liskovich, Yinghai Lu, Yuning Mao, Xavier Martinet, Todor Mihaylov, Pushkar Mishra, Igor Molybog, Yixin Nie, Andrew Poulton, Jeremy Reizenstein, Rashi Rungta, Kalyan Saladi, Alan Schelten, Ruan Silva, Eric Michael Smith, Ranjan Subramanian, Xiaoqing Ellen Tan, Binh Tang, Ross Taylor, Adina Williams, Jian Xiang Kuan, Puxin Xu, Zheng Yan, Iliyan Zarov, Yuchen Zhang, Angela Fan, Melanie Kambadur, Sharan Narang, Aurélien Rodriguez, Robert Stojnic, Sergey Edunov, and Thomas Scialom. Llama 2: Open foundation and fine-tuned chat models. *CoRR*, abs/2307.09288, 2023. doi: 10.48550/ARXIV.2307.09288. URL <https://doi.org/10.48550/arXiv.2307.09288>.
- Matteo Turisini, Giorgio Amati, and Mirko Cestari. LEONARDO: A pan-european pre-exascale supercomputer for HPC and AI applications. *CoRR*, abs/2307.16885, 2023. doi: 10.48550/ARXIV.2307.16885. URL <https://doi.org/10.48550/arXiv.2307.16885>.
- Lucrezia Valeriani, Diego Doimo, Francesca Cuturello, Alessandro Laio, Alessio Ansuini, and Alberto Cazzaniga. The geometry of hidden representations of large transformer models. In Alice Oh, Tristan Naumann, Amir Globerson, Kate Saenko, Moritz Hardt, and Sergey Levine (eds.), *Advances in Neural Information Processing Systems 36: Annual Conference on Neural Information Processing Systems 2023, NeurIPS 2023, New Orleans, LA, USA, December 10 - 16, 2023*, 2023. URL [http://papers.nips.cc/paper\\_files/paper/2023/hash/a0e66093d7168b40246af1cddc025daa-Abstract-Conference.html](http://papers.nips.cc/paper_files/paper/2023/hash/a0e66093d7168b40246af1cddc025daa-Abstract-Conference.html).
- Ashish Vaswani, Noam Shazeer, Niki Parmar, Jakob Uszkoreit, Llion Jones, Aidan N. Gomez, Lukasz Kaiser, and Illia Polosukhin. Attention Is All You Need. *arXiv e-prints*, art. arXiv:1706.03762, June 2017. doi: 10.48550/arXiv.1706.03762.
- Yue Wang, Hung Le, Akhilesh Gotmare, Nghi D. Q. Bui, Junnan Li, and Steven C. H. Hoi. Codet5+: Open code large language models for code understanding and generation. In Houda Bouamor, Juan Pino, and Kalika Bali (eds.), *Proceedings of the 2023 Conference on Empirical Methods in Natural Language Processing, EMNLP 2023, Singapore, December 6-10, 2023*, pp. 1069–1088. Association for Computational Linguistics, 2023. doi: 10.18653/v1/2023.EMNLP-MAIN.68. URL <https://doi.org/10.18653/v1/2023.emnlp-main.68>.
- Benjamin Warner, Antoine Chaffin, Benjamin Clavié, Orion Weller, Oskar Hallström, Said Taghadouini, Alexis Gallagher, Raja Biswas, Faisal Ladhak, Tom Aarsen, Nathan Cooper, Griffin Adams, Jeremy Howard, and Iacopo Poli. Smarter, better, faster, longer: A modern bidirectional encoder for fast, memory efficient, and long context finetuning and inference. *CoRR*, abs/2412.13663, 2024. doi: 10.48550/ARXIV.2412.13663. URL <https://doi.org/10.48550/arXiv.2412.13663>.
- Dejiao Zhang, Wasi Ahmad, Ming Tan, Hantian Ding, Ramesh Nallapati, Dan Roth, Xiaofei Ma, and Bing Xiang. Code Representation Learning At Scale. *arXiv e-prints*, art. arXiv:2402.01935, February 2024. doi: 10.48550/arXiv.2402.01935.

Chen Zhu, Wei Ping, Chaowei Xiao, Mohammad Shoeybi, Tom Goldstein, Anima Anandkumar, and Bryan Catanzaro. Long-short transformer: Efficient transformers for language and vision. In Marc’Aurelio Ranzato, Alina Beygelzimer, Yann N. Dauphin, Percy Liang, and Jennifer Wortman Vaughan (eds.), *Advances in Neural Information Processing Systems 34: Annual Conference on Neural Information Processing Systems 2021, NeurIPS 2021, December 6-14, 2021, virtual*, pp. 17723–17736, 2021. URL <https://proceedings.neurips.cc/paper/2021/hash/9425be43ba92c2b4454ca7bf602efad8-Abstract.html>.

## A Limitations

Due to our dependence on multiple GPUs, we encountered significant computational constraints. Parameter grid searches using smaller and earlier models were the only methods to extrapolate the best hyperparameter setup. The optimal hyperparameters for smaller models can differ from those for larger ones; consequently, we encountered a limitation in discovering an effective training setup. Conducting an ablation study for the in-context classification loss was not practicable due to the high costs of the pre-training stage. Therefore, computational resources pose a significant constraint in this work, and we want to emphasize how this factor can also undermine the possibility of replicating the experiments.

Here, we highlight potential threats to the validity of the research process, focusing on both external and internal factors.

**External validity** When synthesizing the SYNTHCONL code, we rely on code translation; we understand that synthesized data adheres to stylistic writing patterns distinct from those of humans. We tested the model’s performance on standard benchmarks. However, the impact of utilizing code snippets as synthetic data in training large language models for generalization over human text-to-code and code-to-code search is still not fully understood.

**Internal validity** The ablation study focused on fine-tuning the model with and without multi-layer loss. However, this comparison does not account for how the model behaves when starting from a model not pre-trained on multi-layer loss. Although our experiments present promising results, further inspection is necessary to better understand this phenomenon.

## B Synthetic dataset

Table 4: SYNTHCONL composition: Average character count and sample size per language for the CodeSearchNet seed dataset and synthesized portion obtained through translation.

Language	CSN samples	CSN avg. char	Synth. samples	Synth. avg. char
English	1,071,367	180	-	-
PHP	280,706	514	116,967	579
Python	274,454	474	117,374	518
Go	234,089	350	124,125	541
Java	282,118	505	116,098	707
C++	-	-	141,956	938
Ruby	-	-	158,494	456
C	-	-	136,365	1,029
JavaScript	-	-	159,988	557

SYNTHCONL is a fine-tuning dataset designed for text-to-code and code-to-code search, built by augmenting CODESEARCHNET Husain et al. (2019) with transpiled code snippets across multiple languages (Python, Java, Go, PHP, Ruby, C++, C, JavaScript). The dataset underwent a preprocessing phase, including deduplication based on the original and synthesized code columns. Near-deduplication was performed using Locality Sensitive Hashing (LSH) with a Jaccard similarity threshold of 0.7 over character-level 5-grams to remove semantically identical snippets differing only in identifiers or function arguments.

For code-to-code search, we translated each snippet into a randomly sampled target language using the QWEN2.5-CODER-7B-INSTRUCT model with greedy search to ensure consistency. Each dataset entry consists of a natural language description and two code snippets in different languages. SYNTHCONL contains 1,071,367 samples, with original code from CODESEARCHNET (Python, Java, PHP, Go) and translated code (Go, Ruby, JavaScript, Python, C++, PHP, C, Java). In Figure 11, In Figure 12 and Figure 10 some examples of code translation are shown.

Table 4 shows the average number of characters per language in SYNTHCONL, we emphasize that synthesized data is significantly longer than human-written code and might have stylistic differences compared to human code, we further discussed this in the Limitations section.

### C Failure Case Analysis in Code-to-Code Retrieval

<b>PYTHON QUERY</b> <pre>def f_gold(n):     ar = [0] * 10     while (n &gt; 0):         digit = math.floor(n % 10)         if (ar[digit]):             return 0         ar[digit] = 1         n = n / 10     return 1</pre>		<b>JAVA TARGET</b> <pre>static boolean f_gold(int n) {     boolean[] arr = new boolean[10];     for (int i = 0; i &lt; 10; i++) arr[i] = false;     while (n &gt; 0) {         int digit = n % 10;         if (arr[digit]) return false;         arr[digit] = true;         n = n / 10;     }     return true; }</pre>
<b>CodeT5+</b> <b>ERRONIOUSLY RETRIEVED</b> <pre>static boolean f_gold(long n) {     while (n / 100 &gt; 0) {         int last_digit = (int)n % 10;         n /= 10;         n += last_digit * 3;     }     return (n % 29 == 0); }</pre>	<b>UnixCoder</b> <b>ERRONIOUSLY RETRIEVED</b> <pre>static boolean f_gold ( int num ) {     if ( num / 10 == 0 ) return true ;     while ( num != 0 ) {         if ( num / 10 == 0 ) return true ;         int digit1 = num % 10 ;         int digit2 = ( num / 10 ) % 10 ;         if ( Math . abs ( digit2 - digit1 ) &gt; 1 ) return false ;         num = num / 10 ;     }     return true ; }</pre>	<b>ModularStarEncoder - L18</b> <b>ERRONIOUSLY RETRIEVED</b> <pre>static boolean f_gold ( long n ) {     while ( n / 100 &gt; 0 ) {         int last_digit = ( int ) n % 10 ;         n /= 10 ;         n += last_digit * 3 ;     }     return ( n % 29 == 0 ) ; }</pre>
<b>Similarity Score retrieved: 0.88</b> <b>Similarity Score target: 0.83</b>	<b>Similarity Score retrieved: 0.89</b> <b>Similarity Score target: 0.84</b>	<b>Similarity Score retrieved: 0.80</b> <b>Similarity Score target: 0.72</b>

Figure 7: Retrieved incorrect samples from CODET5+, UNIXCODER, and the 18th layer of MOSE. All the models appear to be misled by structural similarities, such as loop functions and return values, highlighting a common superficial retrieval phase.

Table 5: Permutation tests between correct and incorrect similarity scores ( $\alpha = 0.05$ ). The table shows a big discrepancy between MOSE t-statistics and both UNIXCODER and CODET5+ results.

Model	t-statistic	p-value
MOSE (L4)	8.0	<0.001
MOSE (L9)	7.3	<0.001
MOSE (L18)	8.0	<0.001
MOSE (L27)	7.8	<0.001
MOSE (L36)	6.3	<0.001
UNIXCODER	2.2	0.04
CODET5+ 110M-EMBEDDING	2.7	0.009

In this section, we analyzed where our model fails in code-to-code retrieval, relying upon gfg, a Python-to-Java dataset. We compared how our model gets misled by different code snippets with CODET5+ and UNIXCODER, and the confidence level with which the model identifies the occurrences. In fig. 7 we highlight a common defect of the most used open code encoders. When retrieving code snippets focusing on semantic similarity, we emphasize how all the inspected models might get misled by structural factors such as loops, if statements, and return types. The retrieved results underline an overconsideration of structural features despite semantic differences.

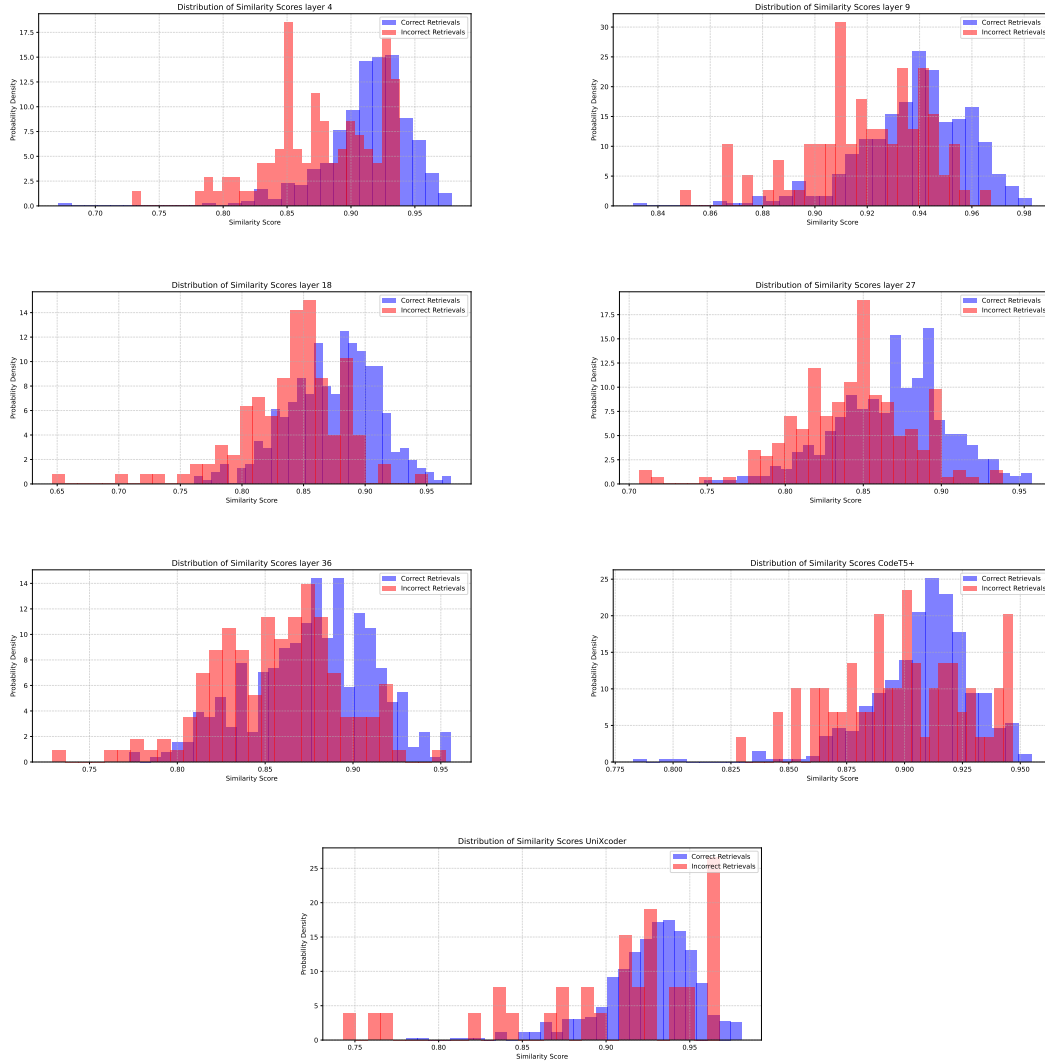


Figure 8: Histograms of normalized similarity score between correct and incorrect retrieved code snippets. The first 5 distributions belong respectively to MOSE 4, 9, 18, 27, 36 layers' exit points; CODET5+ and UNIXCODER are the last ones displayed. While our model tends to have different, distinct distributions regarding wrong and correct retrievals, both UNIXCODER and CODET5+ have more overlapping results.

We then analyzed whether the model's confidence might suggest uncertainty in retrieving incorrect snippets of code, indicating a statistically significant level of "awareness" in overconsidering misleading features. Thus, we compared correct and incorrect similarity distribution scores for retrieved code snippets. Figure 8 shows how MOSE, CODET5+, and UNIXCODER results differ when comparing correct and incorrect retrievals. In table 5, MOSE demonstrated a more significant t-statistic than CODET5+ and UNIXCODER. In a retrieval use case scenario, when the confidence level is insufficient, we suggest that thresholding the similarity score could be an option when deciding whether to provide the end user with a single result or a herd of results.

In fig. 9, we present the differences in similarity scores among the five exit points using a permutation test. It is important to note that, although the model is trained to maintain similar retrieval capabilities across these five exit points (as discussed in section 2.1), and while the incorrectly retrieved snippets might overlap between the layers, each exit point encodes code snippets differently.

Based on these results, we strongly recommend conducting a grid search between the similarity score threshold and the exit point to utilize.

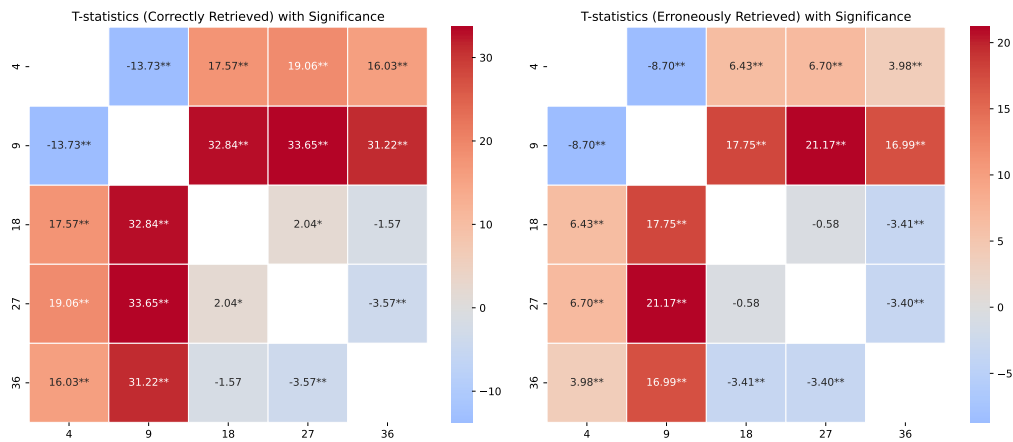


Figure 9: Heatmap of permutation tests (10,000 permutations) between MOSE similarity score results ( $\alpha = 0.05$ ). \* with  $p < 0.05$  and \*\* with  $p < 0.001$ . In the left heatmap, we present the differences in correctly retrieved snippets across various layers, while the right heatmap illustrates the incorrectly retrieved snippets. The heatmaps demonstrate that even layers trained to achieve similar representation objectives can yield different similarity scores.

#### Python

```
def toString(self):
    result = []
    k, v = self.optimalRepr()
    longest = reduce(lambda x, y: x if x > len(y) else len(y), k, 0)
    for ind in range(len(k)):
        result.append("%s : %s" % (k[ind].ljust(longest), v[ind]))
    return "\n".join(result)
```

#### PHP

```
public function toString() {
    /**
     * Return a printable view of the dictionary
     */
    $result = [];
    list($k, $v) = $this->optimalRepr();
    $longest = array_reduce($k, function($x, $y) {
        return $x > strlen($y) ? $x : strlen($y);
    }, 0);
    for ($ind = 0; $ind < count($k); $ind++) {
        $result[] = sprintf("%s : %s", ltrim($k[$ind], ' '), str_pad($v[$ind], $longest, ' ', STR_PAD_LEFT));
    }
    return implode("\n", $result);
}
```

Figure 10: Example of a code snippet translation from *Python* to *PHP*.

## GO

```
// readNextChunk creates an io.LimitedReader for the next chunk of data,
// and returns io.EOF if the last chunk has been read.
func readNextChunk(r wire.SyncScanner) (io.Reader, error) {
    status, err := r.ReadStatus("read-chunk")
    if err != nil {
        if wire.IsAdbServerErrorMatching(err, readFileNotFoundPredicate) {
            return nil, errors.Errorf(errors.FileNotExistError, "no such file or directory")
        }
        return nil, err
    }

    switch status {
    case wire.StatusSyncData:
        return r.ReadBytes()
    case wire.StatusSyncDone:
        return nil, io.EOF
    default:
        return nil, errors.Errorf(
            errors.AssertionError,
            "expected chunk id '%s' or '%s', but got '%s'",
            wire.StatusSyncData, wire.StatusSyncDone, []byte(status),
        )
    }
}
```

## Ruby

```
def read_next_chunk(r)
    status, err = r.read_status("read-chunk")
    if err
        if AdbServerErrorMatching(err, readFileNotFoundPredicate)
            return nil, FileNotExistError.new("no such file or directory")
        end
        return nil, err
    end

    case status
    when wire.StatusSyncData
        return r.read_bytes
    when wire.StatusSyncDone
        return nil, EOFError.new
    else
        return nil, AssertionError.new(
            "expected chunk id '#{wire.StatusSyncData}' or '#{wire.StatusSyncDone}', but got '#{status}'"
        )
    end
end
```

Figure 11: Example of a code snippet translation from *Go* to *Ruby*.

**JAVA**

```
public void get(URI uri, Credentials credentials) throws IOException {  
    get(uri, null, credentials);  
}
```

**C**

```
#include <stdio.h>  
#include <stdlib.h>  
#include <string.h>  
  
typedef struct {  
    char *username;  
    char *password;  
} Credentials;  
  
typedef struct {  
    char *scheme;  
    char *host;  
    int port;  
    char *path;  
} URI;  
  
void get(URI *uri, Credentials *credentials) {  
    // Implementation of the get function  
    printf("Fetching resource from %s://%s:%d%s\n", uri->scheme, uri->host, uri->port, uri->path);  
    if (credentials != NULL) {  
        printf("Using credentials: %s:%s\n", credentials->username, credentials->password);  
    }  
}  
  
int main() {  
    URI uri = {"http", "example.com", 80, "/index.html"};  
    Credentials credentials = {"user", "pass"};  
    get(&uri, &credentials);  
    return 0;  
}
```

Figure 12: Example of a code snippet translation from *Java* to *C*.

## D Model card

Table 6 provides a comprehensive overview of the hyperparameters, architectural choices, and training configurations used in the development of MOSE. This includes detailed settings for both the pre-training and fine-tuning stages, as well as hardware specifications. The information is provided to enhance reproducibility and improve understanding of the model’s design.

Table 6: Details on hyperparameters, architecture, and training for MOSE are presented here, including insights from both pre-training and fine-tuning stages.

Architecture		Pre-training	
Hyperparameter	Value	Hyperparameter	Value
Model size	1B parameters	Batch size	3.99M tokens
Precision	bfloat16	Pretraining steps	245,000
Hidden layers	36	Pretraining tokens	1T
Attention heads	16	Loss function	MLM + In-Context loss
Hidden dimensionality	1,024	Multi-layer loss	Yes
Positional encoding	RoPE ( $\theta = 10^{-6}$ )	Optimizer	AdamW
Context length	2,048	Weight decay	1e-1
Attention mechanism	Grouped Query Attention	Initial learning rate	6.24e-4
Attention pattern	Bi-directional	Learning rate schedule	Multi-step
		Warmup steps	4,000
Fine-tuning		Hardware (Pre-training + Fine-tuning)	
Hyperparameter	Value	Hyperparameter	Value
Dataset size	635,404 samples	Pre-training GPUs	512 NVIDIA Ampere A100 (64GB)
Fine-tuning steps	20,000	Fine-tuning GPUs	512 NVIDIA Ampere A100 (64GB)
Loss function	CLIP loss	Benchmarking GPUs	1 NVIDIA Ampere A100 (64GB)
Multi-layer loss	Yes	Overall training hours	450,000
Batch size	2,048		
Learning rate	1.0e-5		
Temperature parameter	10.0		